An Acad Bras Cienc (2022) 94(Suppl. 1): e20210683 DOI 10.1590/0001-3765202220210683
Anais da Academia Brasileira de Ciências | *Annals of the Brazilian Academy of Sciences*
Printed ISSN 0001-3765 I Online ISSN 1678-2690
www.scielo.br/aabc | www.fb.com/aabcjournal

GEOSCIENCES

An inventory of glacial lakes in the South Shetland Islands (Antarctica): temporal variation and environmental patterns

CARINA PETSCH, KÁTIA K. DA ROSA, MANOELA A.G. DE OLIVEIRA, LUIZ F. VELHO, SABRINA L.C. SILVA, MARIA E. SOTILLE, ROSEMARY VIEIRA & JEFFERSON C. SIMÕES

Abstract: Monitoring and inventorying proglacial lakes in the Maritime Antarctica region is essential for understanding the effects of climate change on these environments. This study uses Landsat images to create a map of lakes in ice-free areas of the South Shetlands Islands (SSI) for 1986/89, 2000/03 and 2020, and verification of patterns of change in lake areas and numbers. Normalized water difference index (NDWI) products, image segmentation, field records, and cartographic products from other studies were used to validate the results. Results show a 60% increase in the number of lakes from 1986/89 to 2000/03; and a 55% increase from 2000/03 to 2020. There was a 52% increase in lake areas from 1986/89 to 2000/03; a 79% increase from 2000/03 to 2020; and a 173% increase from 1986 to 2020. From 1986 to 2020, the most significant changes were a decrease in the average elevation and distance from glaciers and an increase in distance from the sea. In 2020, SSI lakes were predominantly coastal and ice-marginal, with an E and S orientations, flat surfaces, and a low declivity.

Keywords: Climate change, glacier retreat, paraglacial, proglacial environments, Maritime Antarctica.

INTRODUCTION

Glacial lakes are expanding rapidly, and their evolution is connected to glaciers behavior, which, in general, have been retreating due to increasing mean air temperature (Carrivick & Tweed 2013, Wang et al. 2016, Shugar et al. 2020). Global warming exposes over deepened terrain and causes glacial melting, increasing the amount of water available to lakes and raising the number and size of glacial lakes (Che et al. 2004, Chen et al. 2007). Shugar et al. (2020) reported an increase in glacial lake number and total area by 53% and 51%, respectively, in an inventory mapping of glacial lakes worldwide. Hence, inventories of glacial lakes are critical for assessing the influence of climate change on the glacial regime (Raj & Kumar 2016).

The rapid development of remote sensing technologies has driven the monitoring of changes in glacial lakes, mainly due to the vastness of these areas and logistical difficulty in accessing them (Quincey et al. 2007, Wang et al. 2013, Raj & Kumar 2016, Wang et al. 2020). Landsat series is one of the satellites with the most extensive temporal and spatial record for observing Earth's surface, and it provides products suitable for mapping glacial lakes (Nie et al. 2017, Wang et al. 2020). Several authors have successfully used Landsat scenes for this purpose in various parts of the Cryosphere, focusing on the Himalayas in particular. Zhang

et al. (2014; 2015) compiled a list of glacial lakes for the Tibetan plateau (Third Pole); Wang et al. (2014) and Shrestha et al. (2017) for Central Himalayas; Gardelle et al. (2011), Li & Sheng (2012), Nie et al. (2013), Worni et al. (2013), Nie et al. (2017), and Khadka et al. (2018) for the entire Himalayas; Chen et al. (2007) for the Poiqu River sector in Tibet; Wang et al. (2016) for Central Asia; Loriaux & Casassa (2013) for northern Patagonia; and Wang et al. (2020) for the mountainous regions of Asia.

Some glacial lake characteristics are outlined and considered in studies attempting to organize inventories using remote sensing techniques. Some lakes are seasonal - disappearing or freezing at certain times of the year, making a transient and dynamic environment (Carrivick & Tweed 2013, Jawak 2015) - and turbidity modifies reflectance in the visible and near-infrared wavelengths (Gardelle et al. 2011). There is also interference from clouds, mountain shadows, and other sources of error (Sheng et al. 2016). Furthermore, using different data sources and spatial resolutions can lead to inconsistencies when analyzing changes in glacial lakes (Salerno et al. 2012, Nie et al. 2017).

Aside from the inventory, gathering data on lake location, area, and number requires considering the environmental importance of these water bodies in the Antarctic system. Environmental configuration, according to Carriwick & Tweed (2013), has a significant influence on the growth, contraction, filling, emptying, and persistence of the proglacial lakes, which is critical for understanding past environmental conditions and predicting future environmental changes. For the Antarctic Peninsula, Bozkurt et al. (2021) expect an increase in annual-mean near-surface temperatures of about 0.5-1.5 °C for the 2020-2044 period. This temperature increase may cause changes in ice-free areas, leading to new glacial lakes.

Other authors have developed glacial lake inventories in ice-free areas of Maritime Antarctica. In the SSUm, Rosa et al. (2021) and Oliveira et al. (2021) created glacial lake inventories for Nelson and King George Islands (KGI) from 1986 to 2020. However, these studies did not assess the distance between lakes and glaciers or between lakes and the coastline.

These data are critical for understanding environmental evolution and the increase in the number and size of lakes in proglacial areas (i.e., near glaciers) or other parts of the analyzed areas. This study uses Landsat images to create a map of lakes in ice-free areas of the SSI from 1986 to 2020, with subsequent verification of patterns of change in the lake area, number, and location. It investigates the evolution of lakes on each island and between the SSI islands. It addresses the contrasts in the studied period by observing variations in morphometric and spatial parameters. Furthermore, conducting a lake inventory for all ice-free areas of SSI, which has not previously been developed, and presenting a semi-automatic method for lake mapping - allowing researchers to monitor lakes in other sectors with ice-free areas.

MATERIALS AND METHODS

Study area

The SSI is an archipelago located between latitudes 61°S and 63°S, and longitudes 63°W and 53°W. SSI's largest islands are King George, Nelson, Robert, Greenwich, Snow, Low, Deception, Livingston, Smith, Elephant, and Clarence (Ochyra, 1998). This study did not include the northern SSI (*e.g.*, Elephant and Clarence). The Drake Passage separates the archipelago from South America, and the Bransfield Strait separates it from the Antarctic Peninsula (AP) (Figure 1).

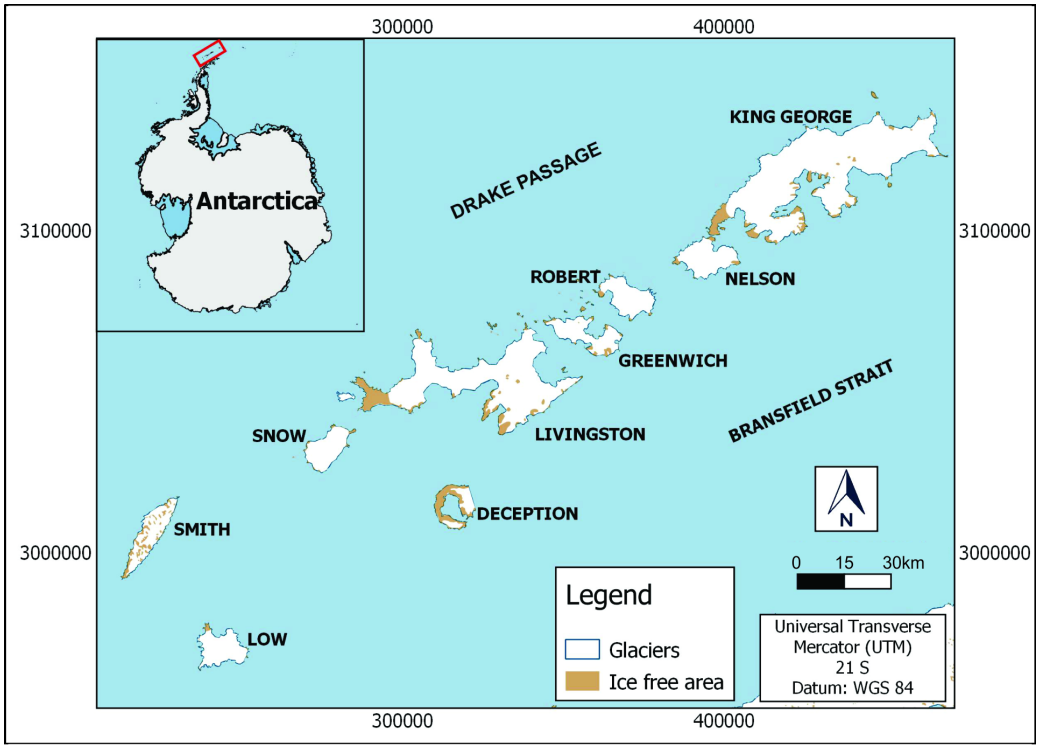

Figure 1. Location of the study area. Basemap data source (Gerrish et al 2020): Antarctic Digital Database (ADD).

The South Shetland Islands are in the Maritime Antarctic region where land is covered by ice caps and permanent snowfields - although some peninsulas, such as Fildes Peninsula in King George Island (KGI) and Byers in Livingstone Island, are free of permanent ice (Watcham et al. 2011). According to Bremer (2008), ice-free areas of SSI are drained by intermittent channels, and morphodynamics is associated with physical and chemical processes caused by snow and ice melting. According to Lopez-Martinez et al. (2012), the Smith (Mt. Foster, 2012 m) and Livingston (Mt. Friesland, 1770 m) islands have mountainous relief, whereas Snow (305 m), Low (180 m), Robert (385 m), and Nelson (332 m) islands have low and flat relief. The authors also note that only 10% of the 4700 km² of raised platforms of marine origin are free of ice.

Several studies have shown glacier retreat on the SSI (Rückamp et al. 2011, Rosa et al. 2015, Simões et al. 2015, Szio & Bialik 2018, Pudelko et al. 2018, Perondi et al. 2020), which has been linked to an increase in air temperature in the AP region from 1948 to the first decades of the 21st century (Vaughan et al. 2003, Turner et al. 2005). The SSI have calving glaciers (Silva et al. 2019). Pudełko et al. (2018) show water-terminating (lake or lagoon) and land-terminating glaciers in King George Island. According to Jonsell et al. (2012), these glaciers are more sensitive to climate change as the ice is near the melting point under pressure.

The annual mean air temperature is -2.8°C, and the austral summer (December to March) mean air temperature is slightly higher than 0°C, with strong winds and high weather variability (Ferron et al. 2004). From 1981 to 2010, the Bellingshausen Antarctic station in KGI had the highest annual mean temperature in the AP (Turner et al. 2020). Although Carrasco (2013), Turner et al. (2016), and Oliva et al. (2017) indicate a regional cooling trend since the late 1990s and early 2000s, Pudełko et al. (2018) recorded changes in annual Positive Degree-Days from

Bellingshausen, Jubany, and Ferraz stations on KGI from 1968 to 2010.

Imagery

The summer season is when there is less snow cover and the water supply is influenced by glacier melting and liquid precipitation - according to Zhang et al. (2015), this configures the best period to make lake inventories - this study uses images acquired on different dates during the austral summers of 1986/89, 2000/03 and 2020, as shown in Table I.

Table I. Images used in lake temporal analysis.

Image	Date	Sensor	Spatial resolution
Landsat 4	01/Mar/1986	TM	30 m
Landsat 4	17/Jan/1988	TM	30 m
Landsat 4	27/Feb/1988	TM	30 m
Landsat 4	28/Jan/1989	TM	30 m
Landsat 4	28/Feb/1989	TM	30 m
Landsat 7	21/Fev/2000	ETM+	30 m
Landsat 7	05/Dec/2001	ETM+	30 m
Landsat 7	30/Jan/2002	ETM+	30 m
Landsat 7	19/Jan/2003	ETM+	30 m
Landsat 7	28/Jan/2003	ETM+	30 m
Landsat 8	19/Jan/2020	OLI	30 m
Landsat 8	09/Feb/2020	OLI	30 m
Landsat 8	03/Mar/2020	OLI	30 m
Landsat 8	12/Jan/2020	OLI	30 m

Digital Elevation Model (DEM)

The DEM used in this study is from the Antarctic Elevation Reference Model (REMA) project (Howat et al. 2019), which is a time-stamped Digital Surface Model (DSM) of Antarctica that includes data from WorldView-1, WorldView-2, and WorldView-3, as well as a small number from GeoEye-1. Data were acquired between 2009 and 2017, with the majority collected during the austral summer seasons of 2015 and 2016. Each REMA DEM is vertically registered to satellite altimetry measurements (Cryosat-2 and ICESat), resulting in absolute uncertainties of less than 1 meter over most areas (Howat et al. 2019). Due to REMA-8 gaps, there are some missing-data pixels in the DEM data. Hence, neighborhood-analysis and interpolation were performed to create a multi-source DEM-derived product (REMA-2 and TanDEM-X DEM) to fill in all no-data values. TanDEM-X, REMA-8, and REMA-2 have high resolution (12 m, 8.8 m, and 2.2 m, respectively) and show high vertical accuracy (RMSE 2.9 m, 0.6 m, and 3.5 m, respectively) (DLR 2019, Howat et al. 2019). The final product is a DEM with an 8-meter spatial resolution.

Field data and supporting materials

During the austral summers of 2013, 2014, 2015, and 2020, four fieldwork campaigns were conducted on King George Island (Admiralty Bay and Fildes Peninsula) and Nelson Island (Harmony Point) to collect lake photographs and GPS coordinates (Figure 2).

Supporting materials are used to verify lake pre-existence and validate polygons whose characteristics do not determine whether the vector generated refers to a lake. SPOT images from 1988 and 2000 (at the end of the summer season) are used to assess lake boundaries and a Sentinel-2 MSI image from 2020. Google Earth's high resolution satellite imagery base map, available in QGIS 4.3 (Zhang et al. 2015, Khadka

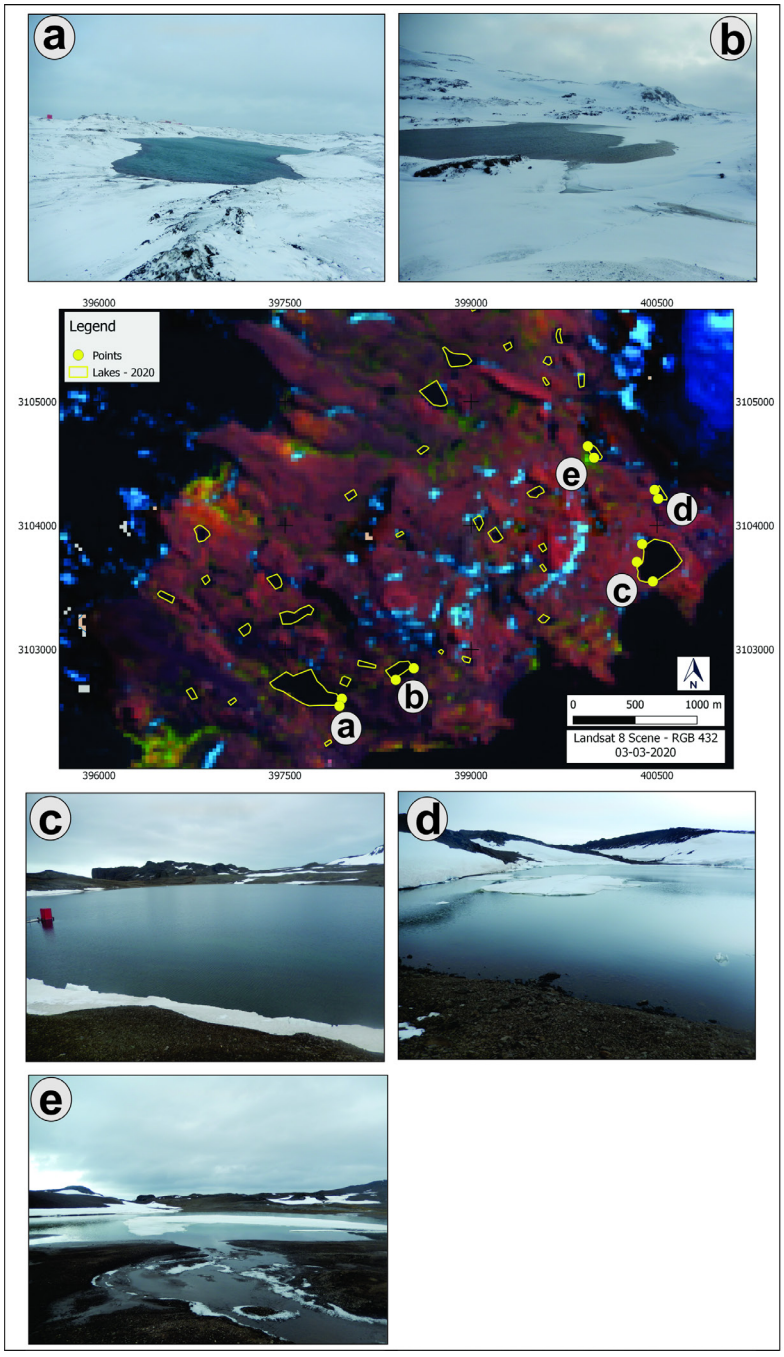

Figure 2. Photographs from field work demonstrating lakes used to validate inventory results.

et al. 2018), is used to visually confirm the presence or absence of a lake feature. Vectors and cartographic products from the Global Land Ice Measurements from Space (GLIMS) project for various SSI ice-free areas (Mink et al. 2014, Rosa et al. 2015, Oliva et al. 2016, Pętlicki et al. 2017, Oliveira et al. 2019, Korczak-Abshire et al. 2019, Perondi et al. 2019, Petsch et al. 2020, Rosa et al. 2021) are used to identify ice-free areas.

Image processing and lake vectoring

Images are pre-processed in the SCP plugin of QGIS 3.4 Geographic Information System, where DOS1 atmospheric correction is used to convert

digital number (DN) values to reflectance. Landsat 8 images are reprojected to the Southern Hemisphere. An error in image registration of ± 0.5 or ± 1 pixel is admitted, with these values being also found by other authors (Gardelle et al. 2011, Nie et al. 2013, Li et al. 2020). Due to clouds in some of the ice-free areas, mosaics of images from different dates are created for the images obtained in the 1980s and 2000 (Nie et al. 2015, Zhang et al. 2015).

In order to detect glacial lakes, all shaded areas in images are removed. A steepest slope > 30% mask is created using DEM data. This masking procedure is essential for eliminating shadow pixels since the spectral response of water is very similar to shadow values recorded by sensors, as demonstrated by Mostafa and Abdelhafiz (2017). The normalized water difference index (NDWI), given by the [(Green - NIR) / (Green + NIR)] formula (McFeeters 1996), is calculated after mask application. Green and NIR wavelengths correspond to B2 and B4 in Landsat TM and ETM+ sensors, and B3 and B5 in the OLI sensor, respectively. NDWI aims to distinguish bodies of water from other land targets (Li et al. 2011), with values ranging from 0.60 to 0.95, usually corresponding to the surface of lakes (Huggel et al. 2002).

Cropped NDWI images are segmented using the region growing method, with a maximum of five iterations and an area of 8 neighboring pixels considered (Rosa et al. 2021). Lakes are then manually vectorized using a combination of segmentation data and color compositions of radiometrically corrected images, yielding a method based on an integrated approach (Huggel et al. 2002, Li et al. 2011, Rai et al. 2017, Khadka et al. 2018, Wang et al. 2020). It should be noted that glacial lakes are identified and edited by one single researcher.

Due to ice and snow-covered lakes, the methodological assumptions of Carrivick & Quincey (2014) are applied in some images, and vector files from the first mapped period (1986/89) are copied to the following period (2020).

Lake vectors are validated using photographs, GPS points, SPOT, Sentinel-2, and Google Earth imagery (section 2.4). The control points obtained in the field (Figure 2a-e) are critical so that vectorization can be performed in other environments due to the similarity of NDWI values and visual interpretation.

Lake spatial interpretation

Following lake mapping, each polygon is labeled with a number (Gardelle et al. 2011) and a set of morphometric and spatial attributes such as elevation, slope, aspect, distance from the glacier, and distance from the ocean are calculated. These parameters are selected because they are the primary determinants of the geomorphological and sedimentary characteristics of the lakes (Rubensdotter & Rosqvist 2009, Carrivick & Tweed 2013), indicating potential causes for changes in the attributes and location of the lakes, and facilitating data interpretation over time. Elevation, slope, and aspect parameters are derived from DEM using QGIS 3.4 software - a 100-meter buffer is created around lakes, and the "basic statistics for numeric fields" tool is used to determine the mean value of each parameter in a given class.

SSI lakes are distributed at elevations ranging from 0 to 250 m, and are therefore divided into five interval ranges: 0-50 m, 50-100 m, 100-150 m, 150-200 m, and 200-250 m. Slope is classified as: 0-2% (flat), 2-5% (gently undulating), 5-15% (undulating), 15-30% (steeply sloping), and 30-45% (very steeply sloping). Interval ranges for orientation angles are defined as: East (45°-135°), South (135°-225°), West (225°-315°), and North (315°-45°).

Spatial parameters - distance from the glacier and distance from the ocean - are divided into distance ranges. The distance to the sea is divided into five intervals: 0-500 m, 500-1000m, 1000-1500 m, 1500-2000 m, and 2000-2500 m. The distance to the glacier is divided into eleven intervals of 500 m due to its greater amplitude, which ranges from 500 to up to 5000 m.

Collected data is subjected to descriptive statistical analyses (frequency tables, measures of central tendency, and variability - mean and standard deviation) to assess the quantity and characteristics of lakes in the studied years, as well as inferential statistical analyses: Kolmogorov-Smirnov Normality test, to support the use of parametric tests; and Student's t-test for independent samples, to assess statistical differences between parameter averages for the 1980s and 2020s (increase or decrease in parameters over the years). All analyses are performed in Microsoft Excel and SPSS v.21 (Statistical Package for Social Sciences, version 21), and for all tests, a significance level of 5% is established. Figure 3 summarizes the methodology used in this study.

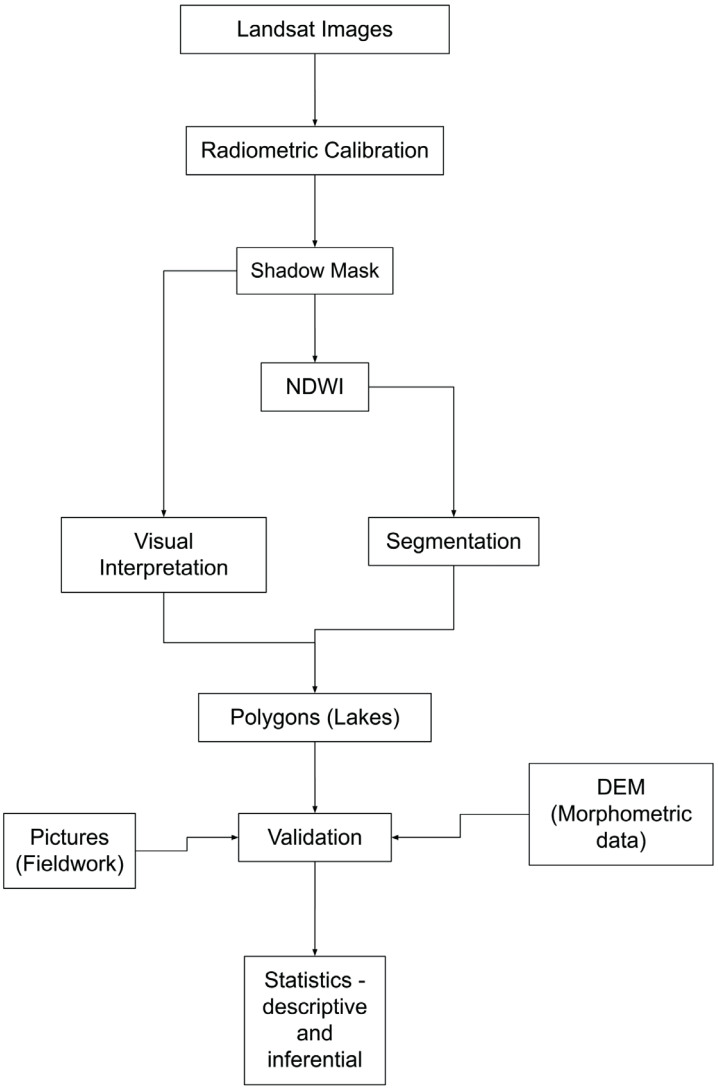

Figure 3. Flowchart of the method used to map the number of lakes and conduct environmental analyses.

RESULTS

Lake identification

Total results for the SSI

For the years 1986/89, 155 lakes are identified by the method, with 84 (54%) obtained by the combination of shadow masking, NDWI, and segmentation (semi-automatic method); and 71 (46%) identified through validation using the supporting materials listed in section 2.4. For the years 2000/03, 248 lakes are identified, with 161 obtained using the semi-automatic method and 87 using validation. For the 2020 image, 385 lakes are identified, with 328 (85%) using the semi-automatic method and 57 using validation. The number of lakes increased by 60% from 1986/89 to 2000/03 and 55% from 2000/03 to 2020. From 1986 to 2020 (34 years of monitoring), the number of lakes increased by 148%.

The total lake area estimated for 1986/89, 2000/03, and 2020 is 1.82 km², 2.77 km², and 4.96 km², respectively. This represents a 52% increase from 1986/89 to 2000/03, and a 79% increase from 2000/03 to 2020. When considering the period from 1986 to 2020, there is a 173% increase. The increase in total area values from 2000/03 to 2020 is greater than from 1986/89 to 2000/03.

Results by islands

Figure 4a-c shows the distribution of lakes across islands and shows the quantities and percentages of area and number of lakes per island in SSI. King George Island has the highest numbers of lakes in all three time periods studied, accounting for 58% (n = 90), 46.3% (n = 115), and 43.8% (n = 169) in 1986, 2000, and 2020, respectively. Livingston Island and Nelson Island are ranked second and third, with Livingston experiencing greater increases in lake numbers over time than Nelson. There are no lakes identified for Smith Island between 1986 and 2020, nor Snow Island in 1986. However, in the 2020 scenario, Snow Island is highlighted as it accounts for 5.71% (n = 22) of the SSI lakes. Considering the variations in numbers of lakes, King George, Robert, Nelson, Deception, and Snow Islands show the greatest increase in absolute value between 2003 and 2020. Low, Livingstone, and Greenwich Islands show the greatest increase in absolute value between 1989 and 2000. And Low Island remains with 4 lakes between 2003 and 2020.

The KGI contains the great majority of lake areas in all scenarios, accounting for 45.5% (0.82 km²), 41% (1.13 km²), and 30.1% (1.49 km²) in 1986/89, 2000/03, and 2020, respectively. Deception and Livingston Islands account for 29.6% (0.53 km²) and 15.7% (0.28 km²) of lake area in 1986/89, respectively; and for 21.9% (0.60 km²) and 20.9% (0.58 km²) in 2000/03, respectively. Livingston Island represents 28% (1.39 km²) of lake area in 2020, comparable to KGI.

Figure 5 shows increases in the absolute number of lakes by island from 1986/89 to 2000/03, and then from 2000/03 to 2020. Results show that from 1986/89 to 2000/03, the three islands with the greatest increases in the absolute number of lakes are: Livingston (33 lakes), King George (25 lakes), and Greenwich (16 lakes). In percentage, the three islands with the highest increases are Livingston (165%), Greenwich (160%), and Nelson (52.6%). From 2000/03 to 2020, the three islands with the greatest increases in absolute data value are King George (54), Nelson (24), and Livingston (20). In percentage, the three islands with the highest increases are Snow (267%), Deception (167%), and Nelson (82.8%).

As for increases in area, the three islands with the greatest increases in total area from 1986/89 to 2000/03 are Livingston (0.32 km²), King George (0.31 km²), and Greenwich (0.12 km²).

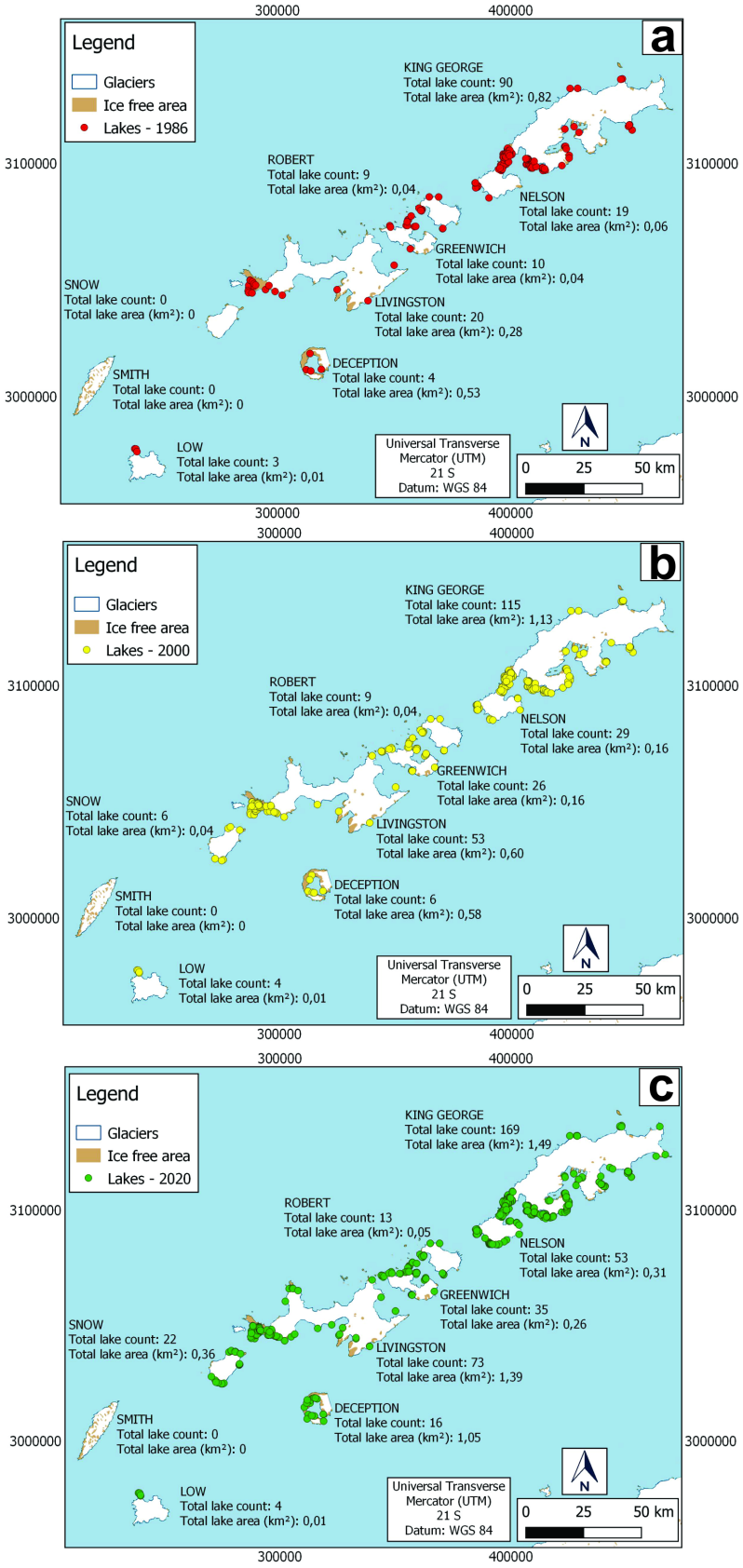

Figure 4. Summary map with data on lake number and area from 1986/89 (a), 2000/03 (b), 2020 (c). Basemap data source: ADD (Gerrish et al 2020). All islands, except for Smith, increased in size and number of lakes.

In percentage, the three islands with the highest increase are Greenwich (300%), Nelson (167%), and Livingston (114%). From 2000/03 to 2020, the three islands with the greatest increase in absolute area value are Livingston (0.79 km²), Deception (0.47 km²), and King George (0.36 km²). In percentage, the three islands with the highest increase are Snow (800%), Livingston (132%), and Nelson (94%). Smith Island has no area values because no lakes are identified in the assessment period. Figure 6 depicts a graph showing the absolute increase in area per island over the two periods analyzed.

Lake location patterns in ice-free areas

In the context of environmental characteristics (Figure 7 and Table II), during 1986/89, more than half of the lakes (51.6%; n = 80) are located at the elevations of 0-50m and 36.1% (n = 56) are between 50-100m. For 2020, 62.6% of the lakes are observed between 0-50m. As for the slope, in 1986/89 there is a predominance of lake occurrence in the 5-15% (36.1%, n = 56) interval, and 29.6% (n = 46) in the 2-5% interval; for 2020, the percentages are similar, with 33.5% of the lakes falling into the 5-15% (n = 129) category, and 29.4% falling into 2-5% (n = 113). As for the aspect, areas around lakes in 1986/89 are mostly facing north (39%, n = 57), whereas in 2020, areas around lakes are mostly facing east (33.5 %, n = 122). Distance from lakes to ocean prevails in the 0-500 m class, accounting for 70.3% (n = 109) in 1986, and 70.9% (n = 273) in 2020. Distance from lakes to glaciers prevails in the 0-500 m interval, accounting 33.3% (n = 50) in 1986; while the 500-1.000 m interval accounts for 14.3% (n = 21), and the 1.000-1.500 m interval accounts for 20.4% (n = 30). In 2020, the lakes are mostly found in the 0-500 m interval (58.3% and n = 218).

Significant differences are observed (Table III) for the elevation data (p-value = 0.045, Student's *t*-test, 5% significance level) with the average being higher in 1989 than in 2020, for distance from the ocean data (p = 0.033) with the average being higher in 2020 than in 1989, and for distance from glaciers data (p-value = 0.043) with the average being higher in 1989 than in 2020.

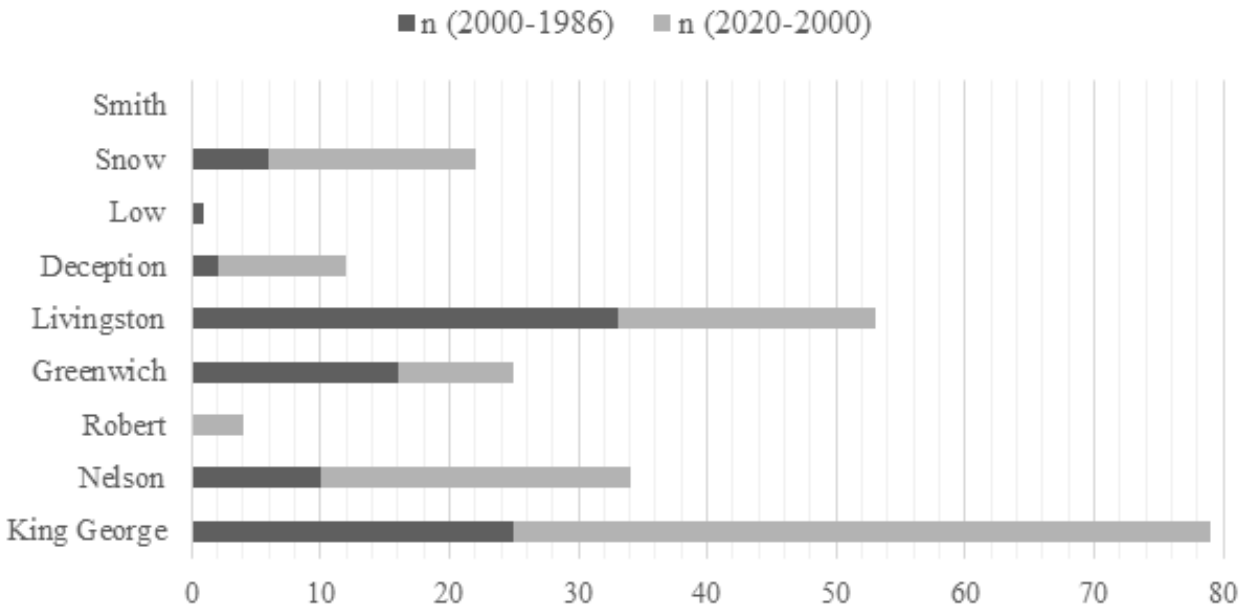

Figure 5. Absolute number of lakes increased between 1986/89 and 2000/03, and between 2000/03 and 2020.

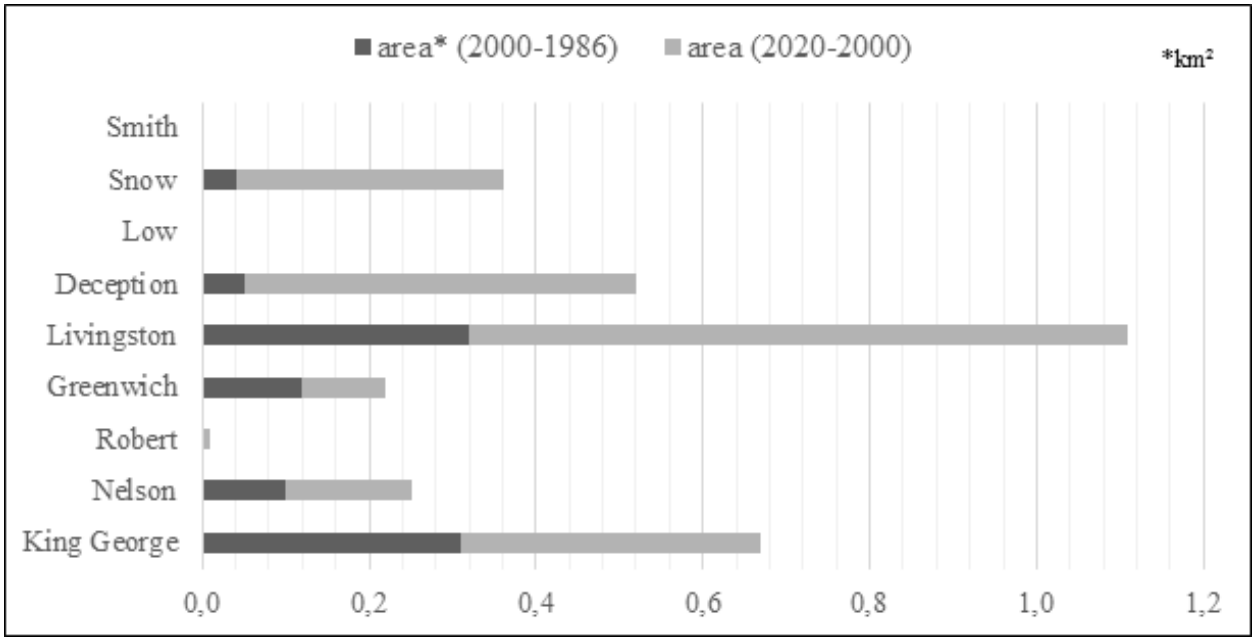

Figure 6. Absolute area increases per island between 1986/89 and 2000/03, and between 2000/03 and 2020.

Lake location patterns in islands

Between 1989 and 2020, lakes were mostly located at elevations lower than 197.6 m. In 2020, lakes began to occur at lower elevations on most islands compared to 1989 (Table IV). Exceptions are Robert and Livingston islands, with more lakes located at higher mean elevation ranges (with little variation) in 2020 than in 1989. When compared to other islands, Deception Island shows the greatest variation in lake location by mean elevation between 1989 and 2000 (Figure 8). Greenwich, Nelson and Robert Islands show the smallest variation in lake location by mean elevation.

As for slope, there is a predominance of lakes located in slopes percentage ranging from 10% to 15% on islands (Figure 8). There are two exceptions: King George and Deception islands, which have lakes in areas with a higher slope than the other islands in 1989 and 2020. Greenwich Island has the greatest variation in lake location by slope class, while Nelson Island has the smallest variation.

Considering the distance from the ocean parameter (Figure 8), the islands of Nelson, Robert, Livingston, and Low are highlighted as they present new lakes located farther away from the coast (1989-2020). When years and locations of lakes are compared, KGI, Deception, and Greenwich islands present lakes with the closest proximity to the coast in 2020. Livingston Island shows the greatest variation in the environmental context in this parameter, followed by Deception Island. Robert Island shows the smallest variation in terms of the distance from the ocean parameter.

When comparing years, the average distance between lakes and glaciers on the islands KGI, Nelson, Deception, Greenwich, Low, and Livingstone has decreased over time. Only Robert Island shows new lakes (2020) that are located further away from glaciers. Lake location on KGI Island varies the most concerning the average distance from the glacier margin (Figure 8).

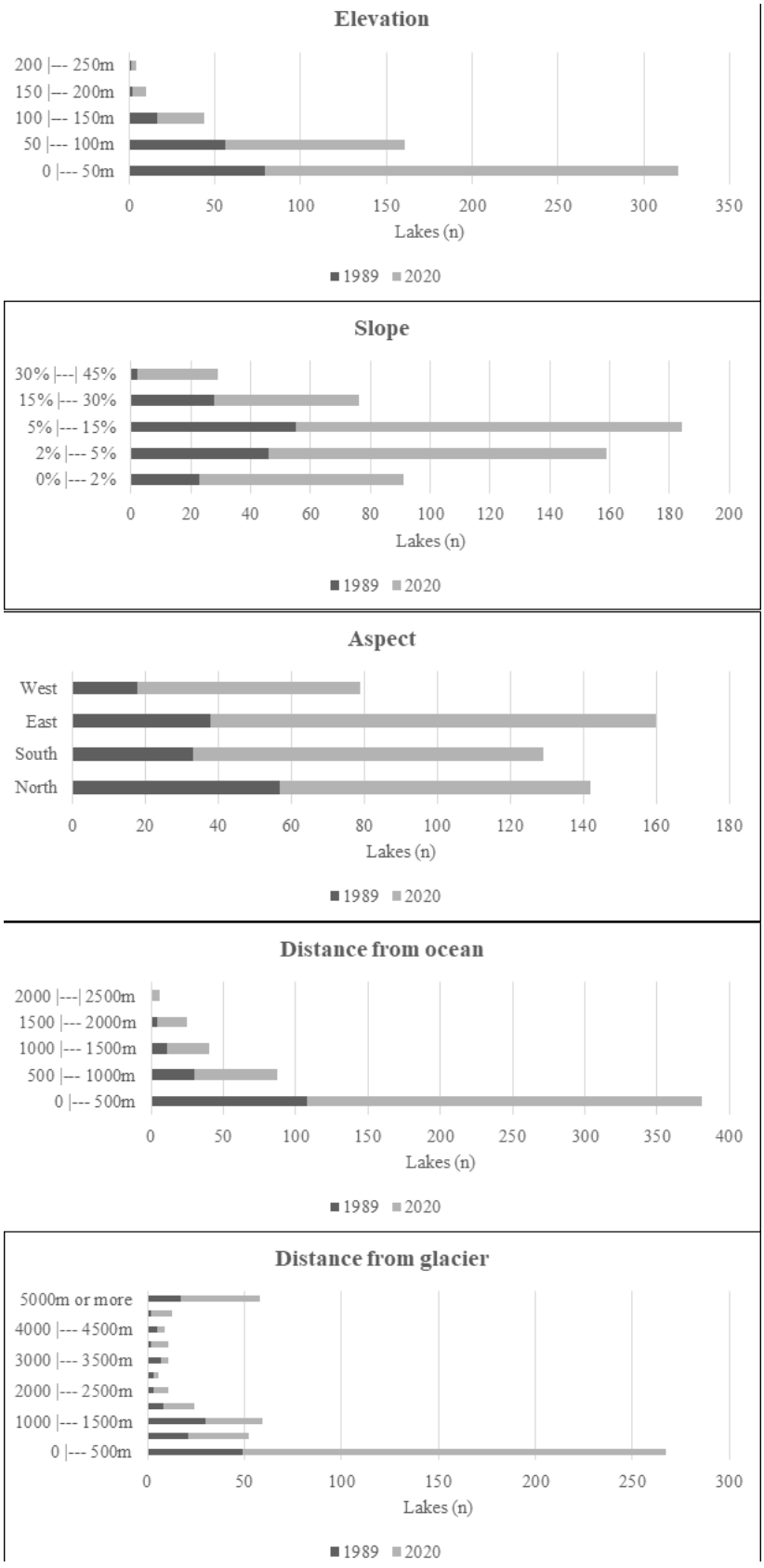

Figure 7. Lake distribution in variables observed (1989-2020) - per island.

Table II. Frequency distribution of the observed variables - by year.

Variable	Year				Variable	Year			
	1989		2020			1989		2020	
	n	%	n	%		n	%	n	%
Elevation (m)					Slope (%)				
0 |--- 50	80	51.6	241	62.6	0% |--- 2%	23	14.8	68	17.7
50 |--- 100	56	36.1	105	27.3	2% |--- 5%	46	29.6	113	29.4
100 |--- 150	16	10.3	28	7.3	5% |--- 15%	56	36.1	129	33.5
150 |--- 200	2	1.2	8	2.1	15% |--- 30%	28	18	48	12.5
200 |--- 250	1	0.6	3	0.8	30% |---| 45%	2	1.2	27	7.0
Total	155	100	385	100	Total	155	100	385	100
Aspect (degrees)					Distance from ocean (m)				
North	57	39.0	85	23.4	0 |--- 500m	109	70.3	273	70.9
South	33	22.6	96	26.4	500 |--- 1000m	30	19.3	57	14.8
East	38	26.0	122	33.5	1000 |--- 1500m	11	7	29	7.5
West	18	12.3	61	16.8	1500 |--- 2000m	4	2.5	21	5.5
Total	146	100	364	100	2000 |---| 2500m	1	0.6	5	1.3
					Total	155	100	385	100
Distance from glacier (m)									
0 |--- 500m	50	33.3	218	58.3					
500 |--- 1000m	21	14.3	31	8.3					
1000 |--- 1500m	30	20.4	29	7.8					
1500 |--- 2000m	8	5.4	16	4.3					
2000 |--- 2500m	3	2.0	8	2.1					
2500 |--- 3000m	3	2.0	3	0.8					
3000 |--- 3500m	7	4.8	4	1.1					
3500 |--- 4000m	2	1.4	9	2.4					
4000 |--- 4500m	5	3.4	4	1.1					
4500 |--- 5000m	2	1.4	11	2.9					
5000m or more	17	11.6	41	11.0					
Total	147	100	374	100					

Table III. Descriptive statistics of the variables and comparisons between the periods observed - years 1989 and 2020. *Standard Deviation. ** significant difference between the means, according to the Student's *t*-test with a 5% significance level.

Variable	Year	n	Mean	SD*	p
Elevation (m)	1989	154	81.8	38.7	0.045 **
	2020	385	75.6	39.2	
Slope (%)	1989	154	13.1	5.0	0.940
	2020	385	13.1	5.6	
Distance from the ocean (m)	1989	154	720.8	466.0	0.033 **
	2020	385	757.1	470.6	
Distance from glacier (m)	1989	147	5744.9	1104.5	0.043 **
	2020	374	4756.7	1246.4	

DISCUSSION

Lake mapping procedure

Shadow masking, image segmentation, and NDWI enabled the identification of most water bodies in the study area, corroborating field monitoring and supporting the visual interpretation of Landsat images. The method identified 54%, 65%, and 85% of the lakes in 1986/89, 2000/03, and 2020, respectively - a result that could be attributed to Landsat 8 OLI sensor enhancements such as resolution and radiometric calibration, signal-to-noise ratio, and a wider range of measurable radiances, which reduces pixel saturation (Morfitt et al. 2015, Loveland & Irons 2016). Furthermore, Fahnestock et al. (2016) note that, compared to the other sensors in the series, Landsat 8 image compilation occurs faster in polar and mountainous environments due to the high image acquisition rate. This enables monitoring both annually and seasonally, demonstrating the evolution of the lakes and the variation in the area as a function of the increase in meltwater and surface thaw. When adding other sources of information to validate the method, an improvement in lake identification is observed. Results also show that the percentage of lakes identified using the semi-automatic method has increased over time, reducing the need for validation, reducing errors, and promoting effective monitoring.

In a dynamic environment with a large spectral mixture of targets, mapping gains from using Landsat 8 OLI images are substantial. Landsat images, however, are limited in their ability to identify small lakes due to their spatial resolution. Thus, given that the vast majority of recent lakes are small, it is noteworthy that the use of Sentinel-2 images may expand the possibility of monitoring lakes in Maritime Antarctica, as several authors have demonstrated the importance of understanding the behavior of proglacial lakes in conjunction with glacier retreat, e.g., Himalayas (King et al. 2019, Watson et al. 2020). Following the assumptions of Gardelle et al. (2011), the smallest glacial lake detected in this study is 4 pixels (0.0036 km²) in size, indicating that our study may have underestimated the number of lakes in the ice-free areas of the South Shetlands.

Table IV. Descriptive statistics for the observed variables - by year and by location.

Place (Island)	Variable	1989		2020	
		Mean	*SD**	*Mean*	*SD**
King George	Hipsometry (m)	197.6	41.3	185.2	45.0
	Slope (%)	43.9	1.6	45.6	1.9
	Distance from the ocean (m)	813.3	395.9	756.2	391.0
	Glacier distance (m)	5891.6	4553.2	4981.5	4924.6
Nelson	Hipsometry (m)	52.8	11.8	51.0	7.1
	Slope (%)	10.0	1.7	10.6	1.6
	Distance from the ocean (m)	583.3	191.7	612.2	210.8
	Glacier distance (m)	2388.9	1036.9	918.4	513.8
Robert	Hipsometry (m)	72.2	26.4	73.1	25.9
	Slope (%)	12.2	3.0	11.2	2.6
	Distance from the ocean (m)	722.2	506.9	730.8	438.5
	Glacier distance (m)	777.8	441.0	807.7	434.9
Greenwich	Hipsometry (m)	50.7	9.8	50.1	5.0
	Slope (%)	3.7	0.8	11.2	2.5
	Distance from the ocean (m)	550.0	50.0	500.0	50.0
	Glacier distance (m)	650.0	100.0	600.0	150.0
Deception	Hipsometry (m)	110.0	5.0	83.3	55.6
	Slope (%)	52.5	1.4	59.0	2.3
	Distance from the ocean (m)	900.0	50.0	700.0	368.4
	Glacier distance (m)	850.0	100.0	750.0	150.0
Low	Hipsometry (m)	69.0	5.0	63.5	10.0
	Slope (%)	13.3	3.1	11.3	1.9
	Distance from the ocean (m)	595.0	100.0	635.0	135.0
	Glacier distance (m)	833.3	577.4	700.0	785.0
Livingston	Hipsometry (m)	68.4	29.9	79.0	34.7
	Slope (%)	10.5	5.2	11.4	5.6
	Distance from the ocean (m)	810.5	586.1	2202.9	704.9
	Glacier distance (m)	3242.1	901.5	1956.5	938.4
Snow	Hipsometry (m)	-	-	86.5	8.9
	Slope (%)	-	-	11.5	1.5
	Distance from the ocean (m)	-	-	764.7	664.2
	Glacier distance (m)	-	-	945.0	135.0

***Standard Deviation.**
Significant reduction in the average, according to Student's t Test to compare independent means with a 5% significance level
Significant increase in the average, according to Student's t Test to compare independent means with a 5% significance level

Wetlands, which are found around lakes and have NDWI values similar to water bodies, add to the complexities of identifying lakes using segmentation and NDWI methods. Therefore, it is recommended that wetlands areas be mapped - an inventory that has yet to be completed for the ISS - and that they are linked to the presence of lakes. This is most evident in portions with the most ice-free areas of SSI as a result of deglaciation processes (John 1972), such as Harmony Point and Stansbury Peninsula (Nelson Island); Fildes, Barton, and Potter Peninsulas (King George Island); and Byers Peninsula (Livingston Island). Lake mapping in these areas is also hampered by shadow interference since their terrain relief is linked to subglacial erosive action. As observed in fieldwork, there are shadows in sectors of cirque valleys, arches, rocky promontories, and U-shaped valleys.

Turbidity may also have hampered lake identification, particularly in areas adjacent to the ice, which have high sedimentary production due to paraglacial activity (Ballantyne 2002) and highlight the rapid evolution of landscapes undergoing glacier shrinkage (Williams & Koppes 2019). In addition to coping with the high cloud cover in the region, which limits satellite image acquisition, proglacial lakes with high sediment input are limiting for semi-automatic vector identification, characterizing this environment as one of the most complex and difficult to map in Maritime Antarctica. As a result, the inventory presented in this research required manual verification, with vectorization of glacial lakes with the aid of high-resolution images available for the study area.

Due to the transience and dynamics of proglacial environments, a satellite image represents only one moment during the ablation period, and the limit of a lake is only an instantaneous state on a given day (Wang et al. 2016, Rosa et al. 2021). Almost all paraglacial landforms and landscapes are transitory (Slaymaker 2009). Therefore, proglacial lakes can expand, coalesce, decrease in size, disappear, or become detached from an ice margin (Carrivick & Quincey 2011).

Increase in the number and area of lakes

Over the 34-year analysis period, the gain in lake number (230 new lakes) and area (3.13 km²) observed represents considerable environmental changes for the ice-free areas of the SSI. Variations in lake area show that the period 2003-2020 was the most significant for the percentage increase in the lake area, while the period 1989-2000 was the most significant for the percentage increase in lake number. It's important to note that there is evidence of an increase in mean air temperature for both periods and evidence of glacier retreat - the formation of new ice-free areas results in environments that are more prone to lake formation.

According to some studies in KGI, for example, a high retreating trend was observed for some glaciers in both periods, and these changes may be related to both the increasing trend of regional average air temperature and the variability of average winter air temperature since the 1980s (Rosa et al. 2021). In recent decades, Rafa et al. (2018) linked glacier area loss to melting degree days in the twentieth and twenty-first centuries in KGI. The year 2020 is highlighted in particular because it sets the record for the highest air temperature in the history of the Antarctic. The WMO recorded a temperature of 18.3°C for the 12 hours (LST) of February 6, 2020, at Base Esperanza in the northern tip of the Antarctic Peninsula, according to Rocha et al. (2021). These changes are most likely associated with an upward trend in annual Positive Degree-Days (Pudełko et al.

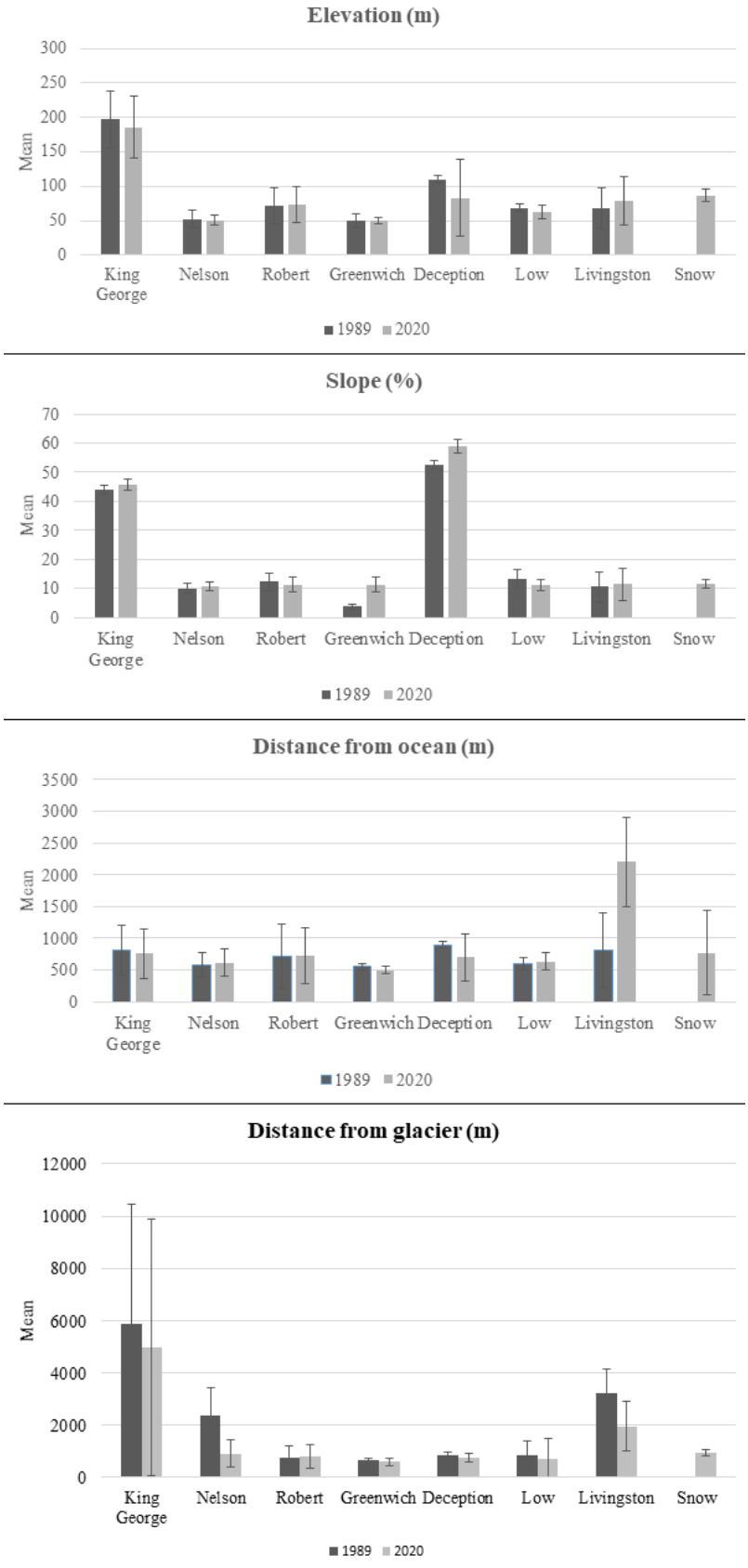

Figure 8. Average values and standard deviation of the parameters assessed (1989-2020) - per island.

2018), as well as an increase in mean surface air temperature (Vaughan et al. 2003, Turner et al. 2005, 2020), and in sea surface temperature - SST (Vaughan 2003) for the Bellingshausen Sea.

It is emphasized that the climatic factor is critical in causing glacier retreat, exposing new ice-free areas, and causing melting to form lakes. Robert, Nelson, and KGI are three specific cases that are examined. Robert Island, despite having an increase of 4 lakes from 2003 to 2020, these are small lakes near the edge of the glacier and in only two ice-free areas that already had lakes in 1989 - demonstrating no abrupt environmental change. Nelson Island, which had lakes in 6 new ice-free portions, and KGI, which has developed 10 new ice-free areas in the period of analysis, all with the presence of newly mapped lakes.

Other studies for the KGI have shown an increase in ice-free areas and marginal and coastal lakes due to glacier retreat. Several studies have shown glacier retreat on the KGI (Rosa et al. 2015, Simões et al. 2015; Perondi et al. 2020). KGI has ice-marginal environments with predominantly flat to gently undulating terrain - in some parts -, which favors the enlargement of lakes over time. This can also be seen in ice-free areas on other islands. Carrivick and Quincey (2014) showed for areas of Greenland that the expansion of the lakes occurs due to the melting of water storage in lakes. One of the consequences of this process, according to the authors, is a reduction in water and sediment supply to the ocean.

KGI, which concentrated most of the lakes in 1986/89 (57.8%), experienced a decrease in value in 2020 (43.9%), indicating the occurrence of important processes such as glacier retreat and the expansion of ice-free areas in the other islands of the South Shetlands. Despite this decrease in lake number proportion, KGI continues to be the island with the most lakes and the greatest increase in lake number (79). Fildes Peninsula, the largest ice-free peninsula in SSI, is located in the KGI and has an ice-free area of approximately 28.8 km² (Andrade et al. 2018). In 2020, Fildes Peninsula alone had 62 lakes, more than any other island in the study area except Livingston (73 lakes).

Livingston Island had the greatest absolute and relative increase in the number of lakes and the greatest absolute increase in area between 1989 and 2000. Between 2000 and 2020, Livingston Island ranked third in total lake growth and first in total area growth. Livingston Island nearly equaled the KGI in terms of area value in 2020. High values of increase in area and number of lakes for Livingston Island are due to the decrease in thickness and shrinkage in glaciers on this island, according to Molina et al. (2007). Furthermore, Byers Peninsula, located in Livingston Island, has been exposed for a long time and is responsible for the variations in distances observed between the lakes and coastline and between lakes and glacier fronts when the 1989-2020 periods are compared.

Results show that Deception, Snow, Greenwich, and Nelson islands also experienced substantial gains in the lake area and/or number. Ice-free areas on these islands may be in topographic areas that allow for the formation of lake basins. Therefore, mapping the evolution of glacier retreat and geomorphological mapping of ice-free areas can aid in understanding the processes that promote lake growth. According to Lopéz-Martinez et al. (2012), the SSI has 33 different types of periglacial relief, demonstrating the great diversity of relief forms and processes in Maritime Antarctica compared to continental Antarctica.

Greenwich Island differs from the others in that it is the only one to show the period 1989-2000 as the greatest gain in absolute lake area - rather than 2000-2020; additionally,

for 1989-2000, Greenwich is the island with the highest percentage of increase in area and the second-highest percentage of gain in number, which is consistent with Stastna (2010). According to Stastna (2010), the Chilean Prat station recorded a rate of increase in mean air temperature of + 0.38 °C per decade for Greenwich Island - which showed the greatest increase in area between 1981 and 2000. Fatras et al. (2020) report 20.4% of the decrease in the area for four glaciers in the north of Greenwich Island between 1956 and 2019, notably the portions that recorded the development of lakes.

Glaciological factors also explain the occurrence of lakes. Islands with no lakes (such as Smith) or few lakes (such as Robert, Low, and Snow) are characterized by ice caps that distinguish them from other islands in the study area. However, Snow Island is highlighted in this lake inventory because it has experienced the most dramatic changes - going from zero to 22 lakes in 34 years. The presence of lakes on Snow Island can alter the sedimentary dynamics of this environment by interfering with the passage of melting water from a glacier and reducing the speed of water flow, resulting in sedimentation of eroded material, according to Carrivick & Tweed (2013).

Morphometric parameter analysis

There is a pattern in lake location in the SSI from 1989 to 2020, with lakes not occupying levels higher than 250 m. Lakes have an average declivity of 13.1%, and they do not occur more than 2500 meters from the coast or more than 10,000 meters from glaciers. For 2020, there are primarily coastal lakes, marginal to the ice, east-oriented, on flat surfaces, and a low percentage of slope in the vicinity of the lake.

The majority of new lakes are proglacial, verified by a decrease in the average distance from glaciers over the years for all islands except Robert. For 2020, most lakes (58.3%) are in recent ice-marginal environments (class 0-500m) formed by changes in terrestrial glaciers. Lakes with the greatest average distances from glaciers are found on KGI, Nelson, and Livingston islands, all of which have significant ice-free areas, as explained in the previous section. On the island of Nelson, the appearance of proglacial lakes in 9 new ice-free areas corroborates the significant decrease in the average distance from the glacier - from 2388.9 m to 918.4 m between 1989 and 2020. However, the predominance of lakes in Harmony Point and Stanbury point has resulted in an increase in the average distance from the glaciers due to the retreat of the ice masses. Therefore, a future analysis by ice-free sectors is recommended for those parameters.

The comparative analysis identified significant changes in distance from the ocean ($p = 0.033$). Data show two trends in terms of the distance between lakes and the coast. There is a rate of increase in the average distance from the coastline, related to glaciers with terrestrial fronts that were retreating (e.g., Nelson, Robert, Low, and Livingston). Compared in time, the lakes of Deception, Greenwich, and KGI were closer to the coast. Oliveira (2021) observed for KGI that tidal-ending glaciers receded faster, causing lakes to form near the shoreline. Such changes can lead to glacier melting and shrinking processes (Jonsell et al. 2012) and the transformation of marine glaciers to non-marine glaciers and new ice-marginal lakes (Perondi et al. 2020, Oliveira et al. 2021).

The increase in lakes in classes above 1000 meters from the ocean may be related to deglaciation processes and landscape evolution of ice-free areas. With the continuation of glacier retreat, the formation of latero-frontal moraines, and changes in the proglacial landforms, lakes can form in areas further away from the ocean

and at higher altitudes. Furthermore, advances in the radiometric resolution of Landsat 8 OLI images may have increased the identification of periglacial lakes, raising the average of lakes farther away from the coastline.

In general, there is a decrease in the average hypsometric (81.8 m to 75.6 m) of lake locations during the 1989-2020 period. Only on the islands of Livingstone, and Robert, the hypsometric mean shows an increase in this period - these islands have lakes further away from sea level (i.e., at lower elevations). Robert Island is also the only one to show an increase in the average distance between lakes and glaciers.

When the slope of the land surrounding the lakes is considered, most of the lakes have slopes ranging from 2 to 15% - as also found by Oliveira et al. (2021). From 1989 to 2020, there were no changes in the average slope value of the areas surrounding the lakes, which remained at 13.1%. Deception Island has the highest slope values, which is explained by its characteristics. The morphology of Deception Island is influenced by two main geomorphological processes - volcanic activity and glacial action, with glaciers covering approximately 57% of the island surface. An almost complete ring of steep hills encircles the sunken interior of Port Foster bay and the outer coast. Thus, melting ice and snow, periglacial activity, slope processes, and the presence of permafrost have also contributed to the formation and evolution of the island relief, with the development of ice streams and lakes that occupy several craters (Smellie et al. 2002).

As for slope orientation, there are changes primarily to north and south for lakes identified in 1986 and to east and west in 2020. According to Andrade et al. (2014), slopes oriented north have higher solar radiation values than slopes facing south. The issue of solar radiation influences the melting of snow and glaciers, resulting in the formation of lakes, but not in the same way that meltwater channels flow, for example, which may explain the formation of lakes in other aspects. Local morphometry issues interfere with meltwater accumulation and lake formation in periglacial environments due to subglacial reliefs, whereas paraglacial processes predominate in proglacial zones, with rapid post-depositional change. Therefore, a DEM from 2016 may not accurately represent either the past or the current proglacial environment.

Given the diverse scenarios presented and the fact that SSI is subjected to similar climatic conditions, the variations may be related to glaciological and environmental factors. Livingston, Greenwich, and Deception have more diverse contexts of location in the parameters assessed. Less variation can be found on islands with more glacial coverage and flatter exposed areas (e.g., Robert & Nelson). In the context of SSI, Perondi et al. (2020), Petsch et al. (2020), and Rosa et al. (2021) have already shown that lake formation is influenced by its location as well as other factors such as glaciers slope, aspect, altitude, and coastline distance, which was also proven in this research.

Understanding the geomorphological scenario in which the lakes are inserted allows for making inferences about glacier retreat patterns and understanding how the ISS proglacial system has evolved and behaved. As ice-free areas are highly vulnerable to climate change, as demonstrated by López-Martinez et al. (2016), their mapping and monitoring should be developed. Furthermore, as the lake inventory proposed in this research may be used to support other studies, knowing the morphometric parameters is essential to make inferences about climate variations (Rubensdotter & Rosqvist 2009); provide the interpretation of processes and reconstructions of past environments and processes (Carrivick & Tweed 2013); and identify 'marginal ice' or

'contact ice' lakes and distal proglacial lakes as they are distinct from each other in terms of geomorphology (Carrivick & Tweed 2013).

CONCLUSION

This first inventory of all lakes located in ice-free areas of the South Shetland Island and their morphometric and spatial parameters, is important because this information can be used in other studies, such as paleoclimatic paleoenvironmental studies. Future research may reveal the impact of the observed changes in the modification of local hydrological flow regimes.

Temporal lake monitoring in SSI, as well as glacier monitoring (Cook et al. 2014), is a challenge due to some factors observed while surveying available satellite images, such as partial or total cloud coverage in the images, lakes with dimensions smaller than those possible to be detected in Landsat images, and the phenology of lakes, which implies the freezing of the liquid surface. Given the limited availability of satellite images, the importance of the inventory and monitoring presented in this study is highlighted since there is a limitation for the inclusion of other periods for temporal monitoring.

Given the difficulty of obtaining optical images as previously stated, the integrative approach proposed in this study, which included satellite image processing products and fieldwork in conjunction with previously published mappings, was vital for the Antarctic environment. Furthermore, the points obtained in the field were critical in allowing validation in some free-of-ice areas and allowing extrapolation to other ISS areas.

Data on lake and area percentage gain shows a considerable amplitude; however, it is noteworthy that all islands show an increase in data. The greater percentage gain and number of lakes in a specific ice-free area represents different hydrosedimentological conditions for the proglacial portions in the face of glacier retreat. Because of large amounts of sediments and meltwater present in paraglacial processes, lake formation usually results in sediment damming and disruption of the transfer of sedimentary material and meltwater to the sea, representing important environmental changes for the area.

As previously documented by other SSI studies, increases in lake number and area are linked to glacier retreat. The decrease in lake predominance in KGI indicates that other islands, such as Deception, Greenwich, Livingston, and Snow, are undergoing pronounced environmental changes, suggesting locations for future research and monitoring.

In general, it is concluded that glacial melting water and the formation of new ice-free areas are the primary sources of the majority of lake expansion and formation from 1986 to 2020. This is because the distance between lakes and glaciers decreased in the year 2020. Furthermore, increases in average distance from the ocean demonstrate that many ice-free areas of the SSI are in different stages of proglacial landscape evolution. These glaciers changed their fronts from marine to land since 1986/89, resulting in the formation of new lakes.

Ultimately, it is emphasized that lake type classification, mapping of fluvial drainage networks in ice-free areas, and investigation of glacial retreat patterns can help to understand better contrasts presented by the values of lake variation per island evidenced in this research. However, such analysis requires the use of higher resolution satellite images and the implementation of additional fieldwork. Changes in slope and orientation of the lake's area suggest that future research should

concentrate on geomorphological analyses of the local relief, associating it with paleo reliefs or paraglacial environments.

Acknowledgments

The Federal Instituto Federal do Rio Grande do Sul (IFRS) supported this study. We also acknowledge the Conselho Nacional de Desenvolvimento Científico e Tecnológico (CNPq) Project 465680/2014-3 (INCT da Criosfera); Coordenação de Aperfeiçoamento de Pessoal de Nível Superior (CAPES); Programa Antártico Brasileiro (PROANTAR); Fundação de Amparo à Pesquisa do Estado do Rio Grande do Sul (FAPERGS) for financial support; UFRGS Pró-Reitoria de Pesquisa e Pós-Graduação (PROPESQ) and UFRGS Graduate Program in Geography. We thank Jeffrey Auger for assistance in language editing.

REFERENCES

ANDRADE AM, ARIGONY-NETO J, POELKING EL, SCHAEFER CEGR, BREMER UF & FERNANDES FILHO EI. 2014. Avaliação da influência da radiação solar na distribuição superficial da vegetação na península Potter, Antártica Marítima. Rev Bras Cartogr 66(1):14-26.

ANDRADE AM, MICHEL RFM, BREMER UF, SCHAEFER CEGR & SIMÕES JC. 2018. Relationship between solar radiation and surface distribution of vegetation in Fildes Peninsula and Ardley Island, Maritime Antarctica. Int J Remote Sens 39: 2238-2254.

BALLANTYNE CK. 2002. Paraglacial geomorphology. Quat Sci Rev 21: 1935-2017.

BIRKENMAJER K, SOLIANI E & KAWASHITA K. 1990. Reliability of Potassium argon dating of Cretaceous Tertiary island-arc volcanic suites of King George Island, South Shetland Islands (West Antarctica). Bull Pol Acad Sci 30: 133-143.

BOLCH T, MENOUNOS B & WHEATE R. 2010. Landsat-based inventory of glaciers in western Canada, 1985-2005. Remote Sens Environ 114(1): 127-137.

BOZKURT D, BROMWICH DH, CARRASCO J & RONDANELLI R. 2021. Temperature and precipitation projections for the Antarctic Peninsula over the next two decades: contrasting global and regional climate model simulations. Clim Dyn. 56: 3853-3874.

CARRASCO JF. 2013. Decadal changes in the near-surface air temperature in the western side of the Antarctic Peninsula. Atmos Clim Sci 3: 275-281.

CARRIVICK JL & QUINCEY DJ. 2014. Progressive increase in number and volume of ice-marginal lakes on the western margin of the Greenland Ice Sheet. Glob Plan Change 116: 156-163.

CARRIVICK JL. 2011. Jökulhlaups: geological importance, deglacial association and hazard management. Geol Today 27: 133-140.

CARRIVICK, JL & TWEED FS. 2013. Proglacial lakes: character, behaviour and geological importance. Quat Sci Rev 78: 34-52.

CHEN X, CUI P, LI Y, YANG Z & QI Y. 2007. Changes in glacial lakes and glaciers of post-1986 in the Poiqu River basin, Nyalam, Xizang (Tibet). Geomorphology 88 (3-4): 298-311.

COOK A, VAUGHAN D, LUCKMAN A & MURRAY T. 2014. A new Antarctic Peninsula glacier basin inventory and observed area changes since the 1940s. Antarct Sci 26(6): 614-624.

COOK AJ, FOX AJ, VAUGHAN DG & FERRIGNO JG. 2005. Retreating Glacier Fronts on the Antarctic Peninsula over the Past Half-Century. Sci 308: 541-544.

COOK AJ, HOLLAND PR, MEREDITH MP, MURRAY T, LUCKMAN A & VAUGHAN DG. 2016. Ocean forcing of glacier retreat in the western Antarctic Peninsula. Science 353 (6296): 283-286.

COOK SJ, KOUGKOULOS I, EDWARDS LA, DORTCH J & HOFFMANN D. 2016. Glacier change and glacial lake outburst flood risk in the Bolivian Andes. Cryosphere 10: 2399-2413.

EMMER A, KLIMEŠ J, MERGILI M, VILÍMEK V & COCHACHIN A. 2016. 882 lakes of the Cordillera Blanca: An inventory, classification, evolution and assessment of susceptibility to outburst floods. Catena 147: 269-279.

FAHNESTOCK M, SCAMBOS T, MOON T, GARDNER A, HARAN T & KLINGER M. 2016. Rapid large-area mapping of ice flow using Landsat 8. Remote Sens of Environ 185: 84-94.

FATRAS C, FERNANDEZ-PALMA BF & MARTILLO C. 2020. Estimating ice retreat on Greenwich island - Antarctica between 1956 and 2019 using optical and SAR imagery. Polar Sci 24: 100526.

FERRON FA, SIMÕES JC, AQUINO FE & SETZER AW. 2004. Air temperature time series for King George Island, Antarctica. Pesqui Antart Bras 4:155-169.

GARDELLE J, ARNAUD Y & BERTHIER E. 2011. Contrasted evolution of glacial lakes along the Hindu Kush Himalaya Mountain range between 1990 and 2009. Glob Planet Change 75: 47-55.

GERRISH L, FRETWELL P, & COOPER P. 2020. High resolution vector polylines of the Antarctic coastline (7.3) UK Polar Data Centre, Natural Environment Research Council, UK

Research & Innovation. Available: https://www.add.scar.org/

GUGLIELMIN M, HRBÁČEK F, ROMAN M, FERNÁNDEZ S, LÓPEZ-MARTÍNEZ J & ANTONIADES D. 2019. Patterns of spatio-temporal paraglacial response in the Antarctic Peninsula region and associated ecological implications. Earth Sci Rev 192: 379-402.

HOWAT IM, PORTER C, SMITH BE, NOH MJ & MORIN, P. 2019. The Reference Elevation Model of Antarctica. Cryosphere 13: 665-674.

HUGGEL C, KÄÄB A, HAEBERLI W, TEYSSEIRE P & PAUL F. 2002. Remote sensing based assessment of hazards from glacier lake outbursts: a case study in the Swiss Alps. Can Geotech J 39: 316-330.

JAWAK SD, KULKARNI K & LUIS AJ. 2015. A Review on Extraction of Lakes from Remotely Sensed Optical Satellite Data with a Special Focus on Cryospheric Lakes. Adv Remote Sens 04(03): 196-213

JOHN BS. 1972. Evidence from the South Shetland Islands towards a glacial history of West Antarctica. In: SUGDEN DE; PRICE RJ. (Eds), Polar Geomorphology, Londres: Institute of British Geographers, p. 75-92.

JONSELL UY, NAVARRO FJ, BAÑÓN M, LAPAZARAN JJ & OTERO J. 2012. Sensitivity of a distributed temperature-radiation index melt model based on AWS observations and surface energy balance fluxes, Hurd Peninsula glaciers, Livingston Island, Antarctica. Cryosphere 6: 539-552.

KHADKA N, ZHANG G & THAKURI S. 2018. Glacial Lakes in the Nepal Himalaya: Inventory and Decadal Dynamics (1977-2017). Remote Sens 10: 1913.

KING O, BHATTACHARYA A, BHAMBRI R & BOLCH T. 2019. Glacial lakes exacerbate Himalayan glacier mass loss. Sci Rep 9: 18145.

KORCZAK-ABSHIRE, M., ZMARZ, A., RODZEWICZ, M, KYCKO M, KARSZNIA I & CHWEDORZEWSKA KJ. 2019. Study of fauna population changes on Penguin Island and Turret Point Oasis (King George Island, Antarctica) using an unmanned aerial vehicle. Polar Biol 42: 217-224.

LEE J, RAYMOND B, BRACEGIRDLE T, CHADÉS I, FULLER RA, SHAW JD & TERAUDS A. 2017. Climate change drives expansion of Antarctic ice-free habitat. Nature 547: 49-54.

LI D, SHANGGUAN D & ANJUM MN. 2020. Glacial lake inventory derived from Landsat 8 OLI in 2016-2018 in China-Pakistan economic corridor. ISPRS Int J Geo-Inf. 9(5): 294.

LI J & SHENG Y. 2012. An automated scheme for glacial lake dynamics mapping using Landsat imagery and digital elevation models: a case study in the Himalayas. Int J Remote Sens 33(16): 5194-5213.

LI J, SHENG Y & LUO J. 2011. Automatic extraction of Himalayan glacial lakes with remote sensing. Remote Sens 15(1): 29-43.

LÓPEZ-MARTÍNEZ J, SCHMID T, SERRANO E, MINK S, NIETO A & GUILLASO S. 2016. Geomorphology and landforms distribution in selected ice-free areas in the South Shetland Islands, Antarctic Northern Peninsula region. Cuad de Investig Geogr 42(2): 435-455.

LÓPEZ-MARTÍNEZ J, SERRANO E, SCHMID T, MINK S & LINÉS C. 2012. Periglacial processes and landforms in the South Shetland Islands (northern Antarctic Peninsula region). Geomorphology 155-156: 62-79.

LORIAUX T & CASASSA G. 2013. Evolution of glacial lakes from the Northern Patagonia Icefield and terrestrial water storage in a sea-level rise context. Glob Planet Change 102: 33-40.

MCFEETERS SK. 1996. The use of the Normalized Difference Water Index (NDWI) in the delineation of open water features. Int J Remote Sens 17 (7): 1425-1432.

MINK S, LÓPEZ-MARTÍNEZ J, MAESTRO A, GARROTE J, ORTEGA JA, SERRANO E, DURÁN JJ & SCHMID T. 2014. Insights into deglaciation of the largest ice-free area in the South Shetland Islands (Antarctica) from quantitative analysis of the drainage system. Geomorphology 225: 4-24.

MOLINA C, NAVARRO F, CALVET J, GARCÍA-SELLÉS D & LAPAZARAN J. 2007. Hurd Peninsula glaciers, Livingston Island, Antarctica, as indicators of regional warming: Ice-volume changes during the period 1956-2000. Ann Glaciol 46: 43-49.

MORFITT R, BARSI J, LEVY R, MARKHAM B, MICIJEVIC E, ONG L, SCARAMUZZA P & VANDERWERFF K. 2015. Landsat-8 Operational Land Imager (OLI) radiometric performance on-orbit. Remote Sens 7: 2208-2237.

MOSTAFA Y & ABDELHAFIZ A. 2017. Shadow Identification in High Resolution Satellite Images in the Presence of Water Regions. Photogrammetric Eng Rem S 83(2): 87-94.

NIE Y, LIU Q & LIU S. 2013. Glacial Lake Expansion in the Central Himalayas by Landsat Images, 1990-2010. PLOS ONE 9(3): e92654.

NIE Y, SHENG Y, LIU Q, LIU L, LIU S, ZHANG Y & SONG C. 2017. A regional-scale assessment of Himalayan glacial lake changes using satellite observations from 1990 to 2015, Remote Sens Environ 189: 1-13.

OCHYRA R. 1998. The moss flora of King George Island. Cracow: Polish Academy of Sciences, 278p.

OLIVA M, ANTONIADES D, GIRALT S, GRANADOS I, PLA-RABES S, TORO M, LIU EJ, SANJURJO J & VIEIRA G. 2016. The Holocene deglaciation of the Byers Peninsula (Livingston Island, Antarctica) based on the dating of lake sedimentary records, Geomorphology 261:89-102.

OLIVEIRA MAG, PETSCH C, ROSA KK, VIEIRA R, COSTA RM, PERONDI C & SIMÕES JC. 2021. Inventário de lagos glaciais nas ilhas Nelson e Rei George, Antártica Marítima, Caminhos de Geografia 22 (80): 119-132.

OLIVEIRA MAG, ROSA KK, VIEIRA R & SIMÕES JC. 2019. Variação de área das geleiras do campo de gelo Kraków, ilha Rei George, Antártica, no período entre 1956 e 2017. Rev Caminh de Geogr 20: 55- 71.

PERONDI C, ROSA KK & VIEIRA R. 2019. Caracterização geomorfológica das áreas livres de gelo na margem leste do campo de gelo Warszawa, Ilha Rei George, Antártica Marítima. Rev Bras Geomorfol 20 (2): 411-426.

PERONDI C, ROSA KK, PETSCH C, IDALINO FD, OLIVEIRA MAG de, LORENZ JL, VIEIRA R & SIMÕES JC. 2020. Recentes alterações nas geleiras e nos sistemas paraglaciais, Antártica Marítima. Rev Geociênc Norde 6(2): 292-301.

PETSCH C, COSTA RM, ROSA KK, VIEIRA R, BRAUN MH & SIMÕES JC. 2020. Desenvolvimento hidrológico e fenologia de lagos da península Fildes - Antártica. Geociênc 39 (2) 559-572.

PUDEŁKO R, ANGIEL P, POTOCKI M, JĘDREJEK A & KOZAK, M. 2018. Fluctuation of Glacial Retreat Rates in the Eastern Part of Warszawa Icefield, King George Island, Antarctica, 1979-2018. Remote Sens 10(6): 892.

QUINCEY DJ, RICHARDSON SD, LUCKMAN A, LUCAS RM, REYNOLDS JM, HAMBREY MJ & GLASSER NF. 2007. Early recognition of glacial lake hazards in the Himalaya using remote sensing datasets. Glob Planet Change 56: 137-152.

RAFAŁ P, ANGIEL P, POTOCKI M, EDREJEK A & KOZAK M. 2018. Fluctuation of glacial retreat rates in the eastern part of Warszawa Icefield, King George Island, Antarctica. Remote Sens. 10(6): 892-900.

RAI PK, MOGAN K, MISHRA S, AHMAD A & MISHRA VN. 2017. A GIS-based approach in drainage morphometric analysis of Kanhar River Basin, India. Appl Water Sci 7: 217-232.

RAJ KBG & KUMAR KV. 2016. Inventory of Glacial Lakes and its Evolution in Uttarakhand Himalaya Using Time Series Satellite Data. J Indian Soc Remote Sens 44: 959-976.

ROCHA FM ET AL. 2021. WMO Evaluation of Two Extreme High Temperatures Occurring in February 2020 for the Antarctic Peninsula Region. Bull Am Meteorol Soc 1-20. (published online ahead of print 2021).

ROSA KK, OLIVEIRA MAG, PETSCH C, AUGER JA, VIEIRA R & SIMÕES JC. 2021. Expansion of glacial lakes on Nelson and King George Islands, Maritime Antarctica, from 1986 to 2020. Geocarto Int: 1-11.

ROSA KK, SARTORI RZ, MENDES JR CW & SIMÕES JC. 2015. Análise das mudanças ambientais da Geleira Viéville, Baía do Almirantado, Ilha Rei George, Antártica. Pesqui Geocienc 42(1): 61-71.

RUBENSDOTTER L & ROSQVIST G. 2009. Influence of geomorphological setting, fluvial, glaciofluvial- and mass-movement processes on sedimentation in alpine lakes. Holocene, 19: 665-678.

RUIZ-FERNÁNDEZ J, OLIVA M, NÝVLT D, CANNONE N, GARCÍA-HERNÁNDEZ C, RÜCKAMP M, BRAUN M, SUCKRO S & BLINDOW N. 2011. Observed glacial changes on the King George Island ice cap, Antarctica, in the last decade, Glob Planet Change 79 (1-2): 99-109.

SALERNO F, THAKURI S, D'AGATA C, SMIRAGLIA C, MANFREDI EC, VIVIANO G & TARTARI G. 2012 Glacial lake distribution in the Mount Everest region: Uncertainty of measurement and conditions of formation. Glob Planet Change 92-93: 30-39.

SEEHAUS T, COOK AJ, SILVA AB & BRAUN M. 2018. Changes in glacier dynamics in the northern Antarctic Peninsula since 1985. Cryosphere 12: 577-594.

SHRESTHA F, GAO X, KHANAL NR, MAHARJAN SB, SHRESTHA RB, WU L, MOOL PK & BAJRACHARYA SR. 2017. Decadal glacial lake changes in the Koshi basin, central Himalaya, from 1977 to 2010, derived from Landsat satellite images. J Mt Sci 14: 1969-1984.

SHUGAR DH, BURR A, HARITASHYA UK, KARGEL JS, WATSON CS, KENNEDY MC, BEVINGTON AR, BETTS RA, HARRISON S & STRATTMAN K. 2020 Rapid worldwide growth of glacial lakes since 1990. Nat Clim Change 10: 939-945.

SILVA BS, ARIGONY-NETO J & BICCA C. 2019. Geomorphological characterization of Antarctic Peninsula glaciers. Rev Bras Geomorfol 20(3): 509-523.

SIMÕES CL, ROSA KK, CZAPELA F, VIEIRA R & SIMOES JC. 2015. Collins Glacier retreat process and regional climatic variations, King George Island, Antarctica. Geogr Rev 105: 462-471.

SLAYMAKER O. 2009. Proglacial, periglacial or paraglacial? Geol Soc Spec Publ 320: 71-84.

SMELLIE JL, LÓPEZ-MARTÍNEZ J, HEADLAND RK, HERNÁNDEZ-CIFUENTES F, MAESTRO A, MILLAR IL, REY J, SERRANO E, SOMOZA L & THOMSON JW. 2002. Geology and Geomorphology of Deception Island. Cambridge, British Antarctic Survey: 77. (BAS Geomap Series, Sheets 6A and 6B).

SMELLIE JL. 1983 Syn-plutonic origin and Tertiary age for the pre-Cambrian False Bay schists of Livingston Island, South Shetland Islands. Antarct Sci 52: 21-32.

STASTNA V. 2010. Spatio-temporal changes in surface air temperature in the region of the northern Antarctic Peninsula and South Shetland islands during 1950-2003. Polar Sci 4: 18-33.

SUDGEN DE & LAPPERTON CM. 1986. Glacial history of the Antarctic Peninsula and South Georgia. S Afr J Sci 82: 508-509.

SZIŁO J & BIALIK R. 2018. Recession and Ice Surface Elevation Changes of Baranowski Glacier and Its Impact on Proglacial Relief (King George Island, West Antarctica). Geosci 8(10): 355.

THOMAS R, LOVELAND J & IRONS R. 2016. Landsat 8: The plans, the reality, and the legacy, Remote Sens Environ 185: 1-6.

TURNER J, COLWELL SR, MARSHALL GJ, LACHLAN-COPE TA, CARLETON AM, JONES PD, LAGUN V, REID PA & IAGOVKINA S. 2005. Antarctic climate change during the last 50 years. Int J Climatol 25: 279-294.

TURNER J, LU H, WHITE I, KING JC, PHILLIPS T, HOSKING JC, BRACEGIRDLE, MARSHALL GJ, MULVANEY R & DEB P. 2016. Absence of 21st century warming on Antarctic Peninsula consistent with natural variability. Nature 535: 411-415.

TURNER J, MARSHALL GJ, CLEM K, COLWELL S, PHILLIPS T & LU H. 2020. Antarctic temperature variability and change from station data. Int J Climatol 40: 2986-3007.

VAUGHAN DG, MARSHALL GJ, CONNOLLEY WM, PARKINSON C, MULVANEY R, HODGSON DA, KING JC, PUDSEY CJ & TURNER J. 2003. Recent Rapid Regional Climate Warming on the Antarctic Peninsula. Clim Change 60: 243-274.

VAUGHAN DG. 2003. Recent rapid regional climate warming on the Antarctic Peninsula, Clim Change 60 (3): 243-274.

WANG X, GUO X, YANG C, LIU Q, WEI J, ZHANG Y, LIU S, ZHANG Y, JIANG Z & TANG Z. 2020. Glacial lake inventory of high-mountain Asia in 1990 and 2018 derived from Landsat images. Earth Syst Sci Data 12: 2169-2182.

WANG X, LIU Q, LIU S, WEI J & JIANG Z. 2016. Heterogeneity of glacial lake expansion and its contrasting signals with climate change in Tarim Basin, Central Asia. Environ Earth Sci 75: 696.

WANG X, LIU SY, MO HW, YAO XJ, JIANG ZL & GUO WQ. 2011. Expansion of glacial lakes and its implication for climate changes in the Chinese Himalayaia. Acta Geogr Sin 144: 104-110.

WANG X, SIEGERT F, ZHOU A & FRANKE J. 2013. Glacier and glacial lake changes and their relationship in the context of climate change, Central Tibetan Plateau 1972-2010. Glob Planet Change 111: 246-257.

WATCHAM EP, BENTLEY MJ, HODGSON DA, ROBERTS SJ, FRETWELL PT, LLOYD JM, LARTER RS, WHITEHOUSE PL, LENG MJ, MONIEN P & MORETON SG. 2011. A new Holocene relative sea level curve for the South Shetland Islands, Antarctica. Quat Sci Rev 30 (21-22): 3152-3170.

WATCHAM EP, HODGSON DA, ROBERTS SJ, FRETWELL PT, LLOYD JM, LARTER RD, WHITEHOUSE PL, LENG MJ & MONIEN P. 2011. A new Holocene relative sea level curve for the South Shetland Islands, Antarctica. Quat Sci Rev 30: 3152-3170.

WATSON SC, KARGEL JS, SHUGAR DH, HARITASHYA UK, SCHIASSI E & FURFARO R. 2020. Mass Loss from calving in Himalayan proglacial lakes. Front. Earth Sci. 7: 342.

WILLIAMS H & KOPPES M. 2019. A comparison of glacial and paraglacial denudation responses to rapid glacial retreat. Ann Glaciol 60(80): 151-164.

WORNI R, HUGGEL C & STOFFEL M. 2013. Glacial lakes in the Indian Himalayas — From an area-wide glacial lake inventory to on-site and modeling based risk assessment of critical glacial lakes, Sci Total Environ 468-469: S71-S84.

YAO X, LIU S, HAN L, SUN M & ZHAO L. 2018. Definition and classification system of glacial lake for inventory and hazards study. J Geogr Sci 28: 193-205.

ZHANG G, YAO T, XIE H, WANG W & YANG W. 2015. An inventory of glacial lakes in the Third Pole region and their changes in response to global warming, Glob Planet Change 131: 148-157.

ZHANG G, YAO T, XIE H, ZHANG K & ZHU F. 2014. Lakes' state and abundance across the Tibetan Plateau. Chin Sci Bull 59: 3010-3021.

SUPPLEMENTARY MATERIAL

Table SI-SII

How to cite

PETSCH C, DA ROSA KK, DE OLIVEIRA MAG, VELHO LF, SILVA SLC & SOTILLE ME, VIEIRA R & SIMÕES JC. 2022. An inventory of glacial lakes in the South Shetland Islands (Antarctica): temporal variation and environmental patterns. An Acad Bras Cienc 94: e20210683. DOI 10.1590/0001-37652022020210683.

Manuscript received on May 01, 2021;
accepted for publication on September 16, 2021

CARINA PETSCH [1,2]
https://orcid.org/0000-0002-1079-0080

KÁTIA K. DA ROSA[2]
https://orcid.org/0000-0003-0977-9658

MANOELA A.G. DE OLIVEIRA[2]
https://orcid.org/0000-0003-1695-1807

LUIZ F. VELHO[2,3]
https://orcid.org/0000-0001-9543-7544

SABRINA L.C. SILVA[3]
https://orcid.org/0000-0001-6791-9036

MARIA E. SOTILLE[2]
https://orcid.org/0000-0002-2965-8004

ROSEMARY VIEIRA[4]
https://orcid.org/0000-0003-0312-2890

JEFFERSON C. SIMÕES[2,5]
https://orcid.org/0000-0001-5555-3401

[1]Universidade Federal de Santa Maria, Departamento de Geociências, Avenida Roraima, 1000, 97105-900 Santa Maria, RS, Brazil

[2]Universidade Federal do Rio Grande do Sul, Centro Polar e Climático, Avenida Bento Gonçalves, 9500, Agronomia, 91501-970 Porto Alegre, RS, Brazil

[3]Instituto Federal de Educação, Ciência e Tecnologia do Rio Grande do Sul/Campus Porto Alegre, Rua Coronel Vicente, 281, Centro Histórico, 90030-040 Porto Alegre, RS, Brazil

[4]Universidade Federal Fluminense, Departamento de Geografia Laboratório de Processos Sedimentares e Ambientais, Campus da Praia Vermelha, Avenida General Milton Tavares de Souza, s/n, 24210-346 Niterói, RJ, Brazil

[5]Climate Change Institute, University of Maine, Orono 04469, ME, USA

Correspondence to: **Carina Petsch**
E-mail: carinapetsch@gmail.com

Author contributions

Carina Petsch: conceptualization, methodology, formal analysis, investigation, writing, reviewing. Kátia Kellem da Rosa: conceptualization, methodology, formal analysis, investigation, writing, reviewing. Manoela Araujo Gonçalves de Oliveira: conceptualization, methodology, investigation. Luiz Felipe Velho: conceptualization, methodology, formal analysis, investigation, writing, reviewing. Sabrina Letícia Couto Silva: conceptualization, methodology, formal analysis, investigation, writing. Maria Eliza Sotille: formal analysis, writing, reviewing, translating. Rosemary Vieira: formal analysis, writing, reviewing. Jefferson Cardia Simões: project administration, reviewing.